

# Importance of backdonation in $[M-(CO)]^{p+}$ complexes isoelectronic to $[Au-(CO)]^+$

C. Gourlaouen,<sup>1,2,3,a)</sup> O. Parisel,<sup>2,3</sup> and J.-P. Piquemal<sup>2,3,a)</sup>

<sup>1</sup>Laboratoire Claude Fréjacques (CEA-CNRS URA 331), CEA/Saclay, DSM/IRAMIS/SIS2M, Bât. 125, 91191 Gif sur Yvette Cedex, France

<sup>2</sup>Laboratoire de Chimie Théorique, UMR 7616, UPMC Université Paris 06, Case Courrier 137, 4 Place Jussieu, F-75005 Paris, France

<sup>3</sup>Laboratoire de Chimie Théorique, UMR 7616, CNRS, Case Courrier 137, 4 Place Jussieu, F-75005 Paris, France

(Received 5 May 2010; accepted 31 August 2010; published online 24 September 2010)

In this contribution, we study several monocarbonyl-metal complexes in order to unravel the contribution of relativistic effects to the metal-ligand bond length and complexation energy. Using scalar density functional theory (DFT) constrained space orbital variation (CSOV) energy decomposition analysis supplemented by all-electron four-component DFT computations, we describe the dependency of relativistic effects on the orbitals involved in the complexation for the  $Au^+$  isoelectronic series, namely, the fully occupied 5d orbitals and the empty 6s orbitals. We retrieve the well-known sensitivity of gold toward relativity. For platinum and gold, the four-component results illustrate the simultaneous relativistic expansion of the 5d orbitals and the contraction of the 6s orbitals. The consequences of such modifications are evidenced by CSOV computations, which show the importance of both donation and backdonation within such complexes. This peculiar synergy fades away with mercury and thallium for which coordination becomes driven by the accepting 6s orbitals only, which makes the corresponding complexes less sensitive toward the relativistic effects. © 2010 American Institute of Physics.

[doi:10.1063/1.3491266]

## I. INTRODUCTION

Relativistic effects are known to play a key role in the coordination properties of gold and are also suspected to be responsible for the liquid state of mercury at ambient temperatures. The cations of Au and Hg are increasingly used in catalysts for organic synthesis and, consequently, theoreticians are more and more confronted by these elements from the viewpoint of inorganic or organometallic chemistry.<sup>1,2</sup> Because of large  $Z$  values, the inner electrons of these elements are subject to relativistic effects, with consequences for the outer electrons involved in chemical bonds: relativity modifies the usual structures of orbitals and disrupts the steady evolution observed for bond lengths and complexation energies of metal-ligand complexes when wandering through the rows and columns of the Periodic Table.<sup>3,4</sup>

Recently, we reported a quantum chemical study on a series of cationic mono-aqua complexes for elements of columns 11 and 12.<sup>5</sup> We retrieved the well-known sensitivity of gold to relativity<sup>3,4</sup> and, to a lesser extent, that of mercury and platinum. As expected, the relativistic effects were found negligible for lighter elements of these columns. A strong correlation was observed between the effects of relativity on the complexation energy and the effects on the cation-ligand bond length.

In this contribution, we consider the more donating car-

bonyl ligand, which is expected to lead to complexes that are more sensitive to the relativistic effects. The considered series of cations includes  $Au^+$ ,  $Hg^{2+}$ , and  $Tl^{3+}$ , all sharing the same valence configuration:  $5d^{10}6s^0$ . In addition, we also will consider neutral platinum (Pt), the theoretical treatment of which is a bit trickier as it exhibits an open-shell  $5d^96s^1$  ground-state electronic configuration. However, all the  $M-CO$  complexes are closed-shell singlet including  $Pt^0CO$ .<sup>6</sup> For the sake of consistency within the investigated series, the bonding energy for  $Pt-CO$  will be computed with respect to the closed-shell  $5d^{10}6s^0$  configuration of the metal.

This contribution is organized as follows: after recalling some methodological procedures and definitions, we will discuss the geometries and the scalar and four-component complexation energies of the carbonyl complexes obtained. These energies will then be analyzed by means of the constrained space orbital variation (CSOV) approach and by Mulliken and natural population analysis (NPA).

## II. METHODOLOGY

### A. Computational details

The all-electron (AE) calculations have been performed using the Faegri's basis set for the cations; such a basis set is known to be of at least double-zeta quality.<sup>7</sup> The four-component calculations have been performed using the DIRAC code.<sup>8-10</sup> The Dirac-Coulomb Hamiltonian<sup>11</sup> has been considered. The uncontracted small component basis sets were generated from the large component sets according to

<sup>a)</sup>Authors to whom correspondence should be addressed. Electronic addresses: christophe.gourlaouen@cea.fr and jpp@lct.jussieu.fr.

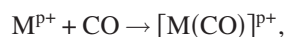
the kinetic balance condition. Finite size Gaussian nuclei were used and the nuclear exponents were taken from a list of recommended values.<sup>12</sup> All (SS/SS) and (SS/LL) integrals have been retained in the calculations. An efficient approximation exists within the DIRAC code<sup>13</sup> for modeling the small component. However, we chose to treat this small component explicitly as our systems were small enough.

The four-component Hamiltonian available in DIRAC allows fully relativistic calculations; hereafter, we will use the following acronyms: FR-RHF/AE for fully relativistic RHF (Restricted Hartree-Fock) computation and FR-DFT/AE for its fully relativistic B3LYP equivalent. Moreover, we also used the nonrelativistic four-component Lévy-Leblond<sup>14</sup> Hamiltonian available in DIRAC; hereafter, denoted as NR-RHF/AE and NR-DFT/AE.

The scalar calculations have been performed using the GAUSSIAN 03 package<sup>15</sup> with the B3LYP<sup>16,17</sup> functional. The standard cc-pVTZ basis set by Dunning<sup>18</sup> was used to describe the C and O atoms. The metallic cations were described by the Def2-TZVP scalar relativistic pseudopotentials by Weigend and Ahlrichs.<sup>19</sup> These pseudopotentials were chosen because they do not involve any H projector (not implemented in all softwares presently used in this study). Mulliken and natural population analysis<sup>20</sup> (NPA) computations were performed at the optimized geometries. Calculations performed with scalar relativistic pseudopotentials will simply be denoted as RHF and B3LYP.

## B. Optimization and interaction energies

Full geometry optimizations have been performed. All complexes have been considered in the  $C_s$  symmetry, allowing M–C–O angle to vary freely. The complexation (binding or formation) energies used hereafter are defined according to the following formation reaction:



$$\Delta E = E([M(CO)]^{P+}) - E(M^{P+}) - E(CO).$$

We have computed the importance of the relativistic and correlation effects on the M–C bond length (quoted D) and complexation energy (quoted E). The nonrelativistic HF calculation (NR-RHF/AE) serves as a reference. We compute the importance of the correlation effects through the following equation:

$$X_c = X(\text{NR-DFT/AE}) - X(\text{NR-RHF/AE}), \quad X = D, E.$$

In the same way, the importance of relativistic effects is defined by

$$X_r = X(\text{FR-RHF/AE}) - X(\text{NR-RHF/AE}).$$

The global contribution of both effects on the two properties is defined by

$$X_{rc} = X(\text{FR-DFT/AE}) - X(\text{NR-RHF/AE}).$$

Finally, we define the synergetic contribution of both effects, which is the interaction between correlation and relativistic effects. It is defined as the global effect on the quantity considered (difference between FR-DFT calculations versus NR-RHF calculation) compared to that of relativistic effects and correlation effects considered separately

$$X_{\text{syn}} = X_{rc} - X_r - X_c.$$

## C. CSOV energy decompositions

Among the different decomposition schemes existing<sup>21–31</sup> (see Ref. 31 for a comparison between schemes), we have retained the CSOV approach, as implemented in our modified version of HONDO95.3.<sup>32,33</sup> The interaction energy  $\Delta E_{AB}$  between two fragments A (here, CO) and B (here,  $M^{P+}$ ) is then split into different components,

$$\Delta E_{AB} = E_1 + E_2 + \delta E,$$

where

$$E_1 = E_{FC},$$

$$E_2 = E_{\text{pol}} + E_{\text{ct}} = E_{\text{polA}} + E_{\text{polB}} + E_{\text{ctA} \rightarrow \text{B}} + E_{\text{ctB} \rightarrow \text{A}}.$$

Here,  $E_1$  ( $E_{\text{frozen core}}$ ) includes the electrostatic and exchange/Pauli repulsion terms.  $E_2$  is the sum of a charge transfer ( $E_{\text{ct}}$ ) term and of a polarization ( $E_{\text{pol}}$ ) term, which can both be split into contributions originating from A and B.  $\delta E$  is implicitly calculated by the first formula. It accounts for some higher-order many-body terms having different physical origins<sup>24,26,34,35</sup> not detailed within the standard CSOV decomposition; they are expected to be small with respect to  $\Delta E_{AB}$ .

Such an approach has been validated within the framework of density functional theory (DFT)<sup>32,36–39</sup> and has recently been extended to pseudopotential calculations on monohydrate cations of heavy elements.<sup>5,40,41</sup> With such an energy decomposition, it can *a priori* be clearly established what is the dominant origin of the complexation energy; this makes then possible to characterize the complex as predominantly *covalent* ( $E_2$  is the largest component in this case) or predominantly *electrostatic* ( $E_1$  is the largest component) species.

It should also be noticed that the  $\Delta E_{AB}$  interaction energy is computed with the fragments frozen in the complex

TABLE I. M–C bond lengths in monocarbonyl complexes (Å).

Basis	Method	[Pt(CO)]	[Au(CO)] <sup>+</sup>	[Hg(CO)] <sup>2+</sup>	[Ti(CO)] <sup>3+</sup>
All-electron	FR-RHF (NR-RHF)	1.828 (2.293)	2.125 (2.665)	2.216 (2.481)	2.228 (2.396)
	FR-DFT (NR-DFT)	1.773 (2.009)	1.938 (2.379)	2.134 (2.383)	2.320 (2.403)
Scalar pseudo	RHF	1.839	2.136	2.223	2.221
Potentials	B3LYP	1.779	1.952	2.145	2.298

TABLE II. C–O bond lengths in monocarbonyl complexes (Å).

Basis	Method	[Pt(CO)]	[Au(CO)] <sup>+</sup>	[Hg(CO)] <sup>2+</sup>	[Tl(CO)] <sup>3+</sup>
All-electron	FR-RHF (NR-RHF)	1.123 (1.115)	1.098 (1.104)	1.090 (1.095)	1.086 (1.088)
	FR-DFT (NR-DFT)	1.158 (1.149)	1.128 (1.126)	1.117 (1.119)	1.121 (1.119)
Scalar pseudo	RHF	1.113	1.090	1.082	1.077
Potentials	B3LYP	1.145	1.116	1.107	1.110

geometry; they are not optimized separately. So, the CSOV procedure will slightly overestimate this quantity.

### III. RESULTS

All complexes adopt a linear  $C_{\infty v}$  symmetry, whatever the cation, the considered charge, or level of calculations. Consequently, this feature will not be discussed further.

#### A. Structure and energy

We report on the variations of the M–C and C–O bond lengths and those of the complexation energies in Tables I–III. Table IV gathers the respective contributions of the relativistic and correlation effects on the complexation energies, the M–C bond lengths, and the synergetic contribution for both effects.

The [Pt(CO)] complex has been subject to numerous experimental<sup>42–46</sup> and theoretical<sup>37,47–53</sup> investigations. The present results are in good agreement with experimental works for bond length: 1.773 Å (FR-DFT/AE) versus 1.760 Å.<sup>44</sup> The [Au(CO)]<sup>+</sup> complex has also been extensively investigated, experimentally.<sup>54–56</sup> Its molecular properties have also been investigated theoretically for its bond properties,<sup>57–59</sup> infrared spectrum,<sup>55,56</sup> and the relativistic effects involved.<sup>40,60</sup> The computed complexation energy is close to the experimental value of 45 kcal mol<sup>-1</sup>.<sup>57</sup> No experimental data are available for [Hg(CO)]<sup>2+</sup> and [Tl(CO)]<sup>3+</sup> and only one theoretical work is available for the mercury complex.<sup>51</sup> The available value of the Hg–C bond length (2.164 Å) is in good agreement with our work, the associated  $\Delta E$  value (–70.0 kcal mol<sup>-1</sup>) is quite smaller than that we found; however, the computational approach is quite different [MP2 level of calculations for the optimization, complexation energy evaluated at the CCSD(T) level].

The present series of complexes is made of heavy elements: platinum (Z=78), gold (Z=79), mercury (Z=80), and thallium (Z=81). For them, the relativistic effects are strong compared to those observed within the lead (Z=82) isoelectronic series,<sup>61</sup> the smallest value is  $D_r = -0.168$  Å for Tl<sup>3+</sup> compared to  $D_r = 0.114$  Å for Tl<sup>+</sup>. Moreover, it is interesting that the distance for Tl<sup>3+</sup> shows a decrease in length with the inclusion of relativity, whereas for Tl<sup>+</sup>, this effect is reversed.

We partially retrieve the usual “gold effects”<sup>4</sup> for bond lengths: the relativistic effects are strong for platinum, increase for gold, and then decrease up to thallium. On the contrary, the influence on the complexation energies, in absolute values, decreases from platinum to gold and then increases up to thallium;  $E_r = -12.6$  kcal mol<sup>-1</sup> for Au<sup>+</sup> and –39.1 kcal mol<sup>-1</sup> for Tl<sup>3+</sup>. Nevertheless, the contribution of the relativistic effects to the net complexation energies tends to decrease slightly, amounting to 25% for gold and to 22% for thallium. It seems then that the particular sensitivity of gold toward relativistic effects is large with respect to geometry, but is less pronounced for the complexation energy.

For this series, both correlation and relativistic effects tend to shorten the bond length and stabilize the complex. The one-component HF calculation leads to the expected increase of the complexation energy from platinum to thallium as, at the same time, the M–C bond length decreases (except for platinum). It is in good agreement with the “rule of thumb” that the most charged metal should lead to the shortest metal-CO bond length and to the most stable complex. If trends for complexation energies are not affected by any of the relativistic or correlation effects, they are for bond lengths.

Upon inclusion of correlation effects, M–C bond lengths are similar for Au<sup>+</sup>, Hg<sup>2+</sup>, and Tl<sup>3+</sup>. However, the order is reversed compared to the one-component HF calculation: the Au–C bond length is now shorter than of Tl–C. The relativistic effects lead to a spectacular decrease of the Au–C bond length by 0.540 Å and by 0.465 Å for Pt–C, but only by 0.265 Å for Hg–C and by 0.168 Å for Tl–C. The combination of the two effects, relativity and correlation, leads to a bond length increase of roughly 0.2 Å from platinum to thallium, contrary to what could have been expected: the most charged complex has the longer bond length.

#### B. Population analysis and energy decompositions

The NPA shows the evolution of the cationic orbital populations. Many points arise from Table V. The main point is the population of the 5d orbitals, which decreases from mercury to platinum. The d shells of Hg<sup>2+</sup> and Tl<sup>3+</sup> are full, whereas a significant population is missing for Pt. The situ-

TABLE III. Complexation energies ( $\Delta E$  in kcal mol<sup>-1</sup>). All fragments and complexes are taken into their singlet closed-shell state.

Basis	Method	[Pt(CO)]	[Au(CO)] <sup>+</sup>	[Hg(CO)] <sup>2+</sup>	[Tl(CO)] <sup>3+</sup>
All electrons	FR-RHF (NR-RHF)	–44.0 (–2.1)	–20.4 (–7.8)	–50.8 (–31.4)	–122.2 (–83.0)
	FR-DFT (NR-DFT)	–85.3 (–27.0)	–49.9 (–17.8)	–82.3 (–49.1)	–174.4 (–116.1)
Scalar pseudo	RHF	–39.9	–20.4	–52.3	–125.5
Potentials	B3LYP	–78.2	–48.1	–82.6	–175.4

TABLE IV. Respective contribution of relativity and correlation to the M–C bond length (Å) and to the complexation energy (kcal mol<sup>-1</sup>).

Method	[Pt(CO)]	[Au(CO)] <sup>+</sup>	[Hg(CO)] <sup>2+</sup>	[Tl(CO)] <sup>3+</sup>
D <sub>r</sub>	-0.465	-0.540	-0.265	-0.168
E <sub>r</sub>	-41.8	-12.6	-19.4	-39.1
D <sub>c</sub>	-0.284	-0.286	-0.098	0.007
E <sub>c</sub>	-24.9	-10.0	-17.6	-33.1
D <sub>rc</sub>	-0.520	-0.727	-0.347	-0.076
E <sub>rc</sub>	-83.1	-42.1	-50.9	-91.4
D <sub>syn</sub>	0.229	0.099	0.016	0.085
E <sub>syn</sub>	-16.4	-19.5	-13.9	-19.2

ation of Au<sup>+</sup> is intermediate; the RHF value, however, suggests that the decrease in the population is not an artifact. We must then consider the eventuality of the existence of backdonation from the cation toward the empty  $\pi^*$  orbital of the carbonyl. The evolution of the 6s orbital population is much more complicated; it decreases from Pt to Hg<sup>2+</sup> and then increases to Tl<sup>3+</sup>. We will discuss this point later. Finally, as could have been expected, the net charge transfer from the carbonyl to the cation increases from Pt (0.11 electron) to Tl<sup>3+</sup> (0.68 electron).

To complete the analysis of the complexes, we performed binding energy decompositions. As discussed in Sec. II, the energy is decomposed into six terms, which will be discussed in the following. E<sub>1</sub> is strongly repulsive for Pt and Au<sup>+</sup> and quasinil for Hg<sup>2+</sup> and Tl<sup>3+</sup>. To compute this term, the orbitals of the fragment are optimized separately and then frozen. The final orbitals of the complex are formed from the orthogonalized monomer orbitals without any global reoptimization. Consequently, it merges the Coulomb interaction (electrostatic) to the exchange-repulsion (Pauli) between the occupied orbitals of the isolated fragments.<sup>33</sup> This shows that the Coulombic attraction between the cation and CO does not ensure, solely, the stability of these complexes and that the exchange-repulsion is predominant. This can be interpreted as a penetration of the lone pair of CO into the occupied orbitals of the cation, as suggested by the very short distance observed between CO and Pt or Au<sup>+</sup>.

The second-order term E<sub>2</sub> decreases from Pt to Hg<sup>2+</sup> and then increases for Tl<sup>3+</sup>. A rough analysis is difficult and we have then to consider the individual contributions.

The metal polarization and the backdonation (charge transfer from the metal to the CO ligand) terms decrease monotonously from Pt to Tl<sup>3+</sup>. This is consistent with the NPA as the population of the 5d orbitals increases from Pt to Hg<sup>2+</sup> and Tl<sup>3+</sup> for which they are full—proof of the absence

TABLE V. NPA of the 5d and 6s orbitals and net charge of the cations.

Method		[Pt(CO)]	[Au(CO)] <sup>+</sup>	[Hg(CO)] <sup>2+</sup>	[Tl(CO)] <sup>3+</sup>
RHF	5d	9.40	9.89	9.97	10.0
	6s	0.68	0.21	0.21	0.41
	Net charge	-0.09	0.88	1.79	2.57
B3LYP	5d	9.18	9.73	9.94	10.0
	6s	0.94	0.49	0.40	0.68
	Net charge	-0.11	0.78	1.64	2.32

TABLE VI. Energy gap between the 5d<sub>5/2</sub> and 6s<sub>1/2</sub> spinors (a.u.) in the isolated cations.

Method	Pt	Au <sup>+</sup>	Hg <sup>2+</sup>	Tl <sup>3+</sup>
FR-RHF (NR-RHF)	0.300 (0.375)	0.465 (0.587)	0.643 (0.815)	0.832 (1.057)
FR-DFT (NR-DFT)	0.030 (0.119)	0.136 (0.269)	0.261 (0.442)	0.406 (0.638)

of backdonation. The CSOV analysis confirms that the partial weakening of the 5d population is due to backdonation and not to 5d-6s transfer.

The polarization of CO and its donation to the cation are more difficult to interpret and the results for the Pt complex are noticeable. For this complex, the  $\delta E$  term (i.e., the energy not taken into account within the CSOV contributions) is very large, whereas it is expected to remain small.<sup>31,33,35</sup> This is a hint toward showing that the CSOV description is not well suited to the description of such a covalent complex. Otherwise, the polarization of the carbonyl increases steadily from Au<sup>+</sup> to Tl<sup>3+</sup>, in agreement with the strength of the electric field generated by the cation. The donation term also increases; however, it is quasi-identical for Au<sup>+</sup> and Hg<sup>2+</sup> despite the greater charge held by the cation. This is again in line with the similar population of the 6s orbital given by the NPA for both cations.

## IV. DISCUSSION

Both NPA and CSOV decomposition results have put in evidence the role played by the 5d orbitals in Pt and Au<sup>+</sup> complexes through backdonation. The donation toward the 6s orbital increases simultaneously with the M–C bond length. It shows that, alone, donation is not the driving force of the binding, as the bond elongation should disfavor it. Our conclusion is that the characteristics of the complexes are the result of the balance between the two terms: donation to the 6s and backdonation from the 5d.

The characteristics of the CO fragment are constant, so they could not be the source of the differences between the complexes. Three parameters are then to be considered: the charge of the cation, the donation, and the backdonation. We have already shown that the charge held by the cation leads to the exact opposite evolution of the complexes' characteristics when taking into account the relativistic effects. This suggests that it has no direct influence at least on the bond lengths.

Relativistic effects modify the energy of the orbitals. The capacity of the 5d orbitals to donate electron to the vacant orbitals of the carbonyl and that of the 6s to accept electrons from the full orbitals of the ligand are directly linked to the relative energy difference between the 5d, the 6s, and the ligand orbitals. As relativistic (and correlation) effects modify these energies, this donation capacity will be directly affected by this effect.

In Table VI, we have reported the energy gap between the 5d and the 6s orbitals of the cations. It is noticeable that the relativistic and correlation effects both tend to diminish this gap, and that the lower this gap is, the shorter is the M–C

TABLE VII. Mulliken population of large (L) and small (S) components of the cations.

Method		[Pt(CO)]	[Au(CO)] <sup>+</sup>	[Hg(CO)] <sup>2+</sup>	[Tl(CO)] <sup>3+</sup>
NR-RHF	L	77.845	78.007	78.071	78.425
	L	77.265	77.549	77.675	78.113
FR-RHF	S	0.491	0.502	0.523	0.540
	L+S	77.755	78.051	78.198	78.652
NR-DFT	L	77.653	78.031	78.169	78.597
	L	77.354	77.612	77.838	78.308
FR-DFT	S	0.493	0.502	0.523	0.540
	L+S	77.847	78.114	78.361	78.848

bond length. The gap is a good picture of the backdonation ability of the 5d orbitals. Their quick stabilization from Pt to Tl is illustrated by the increasing gap up to Tl for which the 5d electrons are not involved in the binding, as illustrated by the CSOV and NPA. A last clue on the origin of the M–C bond length evolution is given by the radii of the different 5d and 6s orbitals, as calculated by Desclaux on the neutral atoms.<sup>4</sup> There is a stronger contraction of the 6s<sub>1/2</sub> spinor from Pt to Tl (0.388 bohr) compared to that of the 5d<sub>5/2</sub> (0.150 bohr). Furthermore, the radius of the 5d<sub>5/2</sub> spinor is one-half that of the 6s<sub>1/2</sub>.

A consistent scheme arises from all these elements. By reducing the energy gap, correlation and relativistic effects favor backdonation from the 5d orbitals. However, to maximize the overlap between these orbitals and the accepting CO  $\pi^*$ , the outer-ligand orbitals have to penetrate into the 6s shell to get closer to the 5d orbital. At the same time, this empty 6s shell is partially populated by donation from the ligand. The result is a competition. On one hand, the bond length tends to shorten in order to maximize the overlap between the ligand and the 5d orbital of the cation. On the other hand, the bond length tends to lengthen in order to diminish the repulsion between the ligand and the partially occupied 6s shell and the full 5d shell of the cation. Of course, one should keep in mind that DFT usually gives a smaller gap than HF and post-HF methods, leading to an overestimation of charge transfer.<sup>33</sup> Nevertheless, the observed backdonation effects remain present at the HF level, which does not suffer from usual self-interaction DFT artifact linked to the HOMO-LUMO (highest energy occupied molecular orbital-lowest energy occupied molecular orbital) gap problem.

We can now explain the amplitude of the relativistic effects on the complexes. For platinum, the 5d orbitals are already high enough in energy at the RHF level to allow backdonation: it is the only electron deficient fragment in the series (see Mulliken populations in Table VII). The relativistic effects expand the 5d and contract the 6s (see Ref. 62) orbitals: this reinforces backdonation as illustrated by a greater electron deficiency. The main orbitals to consider are the 5d orbitals, which are less sensitive to the relativistic effects than the 6s (see the table in Supplementary Material). For Hg and Tl, the complex is governed by donation to the 6s orbitals (Table VIII). Consequently, the amplitude of the relativistic effects on the complex depends on their influence on this orbital. The relativistic contraction of the 6s orbital

TABLE VIII. Energy decompositions at the RHF/DEF2 level (kcal mol<sup>-1</sup>).

	[Pt(CO)]	[Au(CO)] <sup>+</sup>	[Hg(CO)] <sup>2+</sup>	[Tl(CO)] <sup>3+</sup>
$\Delta E_{AB}$	-40.4	-21.0	-53.4	-126.9
E <sub>1</sub>	130.0	29.9	9.6	2.1
E <sub>2</sub>	-149.9	-48.9	-62.9	-128.8
$\delta E$	-20.5	-1.9	-0.4	-0.3
Cation polarization	-41.9	-10.5	-5.7	-5.9
CT: cation to CO	-40.0	-6.6	-1.6	-0.6
CO polarization	-24.8	-10.5	-31.2	-69.6
CT: CO to cation	-43.2	-21.3	-24.1	-52.6

decreases from gold to thallium. It is explained easily; the increasing charge of the nucleus already contracts the 6s orbital at the RHF level, so the supplementary contraction due to the relativistic effects can only decrease as the inner shells contraction is much smaller than that of the 6s orbitals (see Ref. 62); in that way, the electron repulsion rapidly increases. This is why the relativistic effects are smaller on Tl than on Hg for the M–C bond lengths.

The last case to treat is gold. The larger contribution of relativistic effects on the Au–C bond length is due to the contraction of the 6s orbital, which is important enough to allow the ligand to interact with the 5d orbitals. This favors the penetration of the C lone pair of the CO within the partially occupied 6s cation orbital. This is possible despite the electron repulsion with the partially occupied 6s orbital as it maximizes the overlap between the 5d orbital of gold and the orbital of the ligand. This repulsion between the orbitals is illustrated by the highly repulsive value of the frozen core (E<sub>1</sub>) interactions (see Table IX). So for gold, relativistic effects not only increase donation toward the ligand but also create the conditions to allow backdonation, conditions that are not present at the nonrelativistic level.

## V. CONCLUSIONS

By means of different series of monocarbonyl-metal complexes, we have explored the evolution of the contribution of the relativistic effects to the metal-ligand bond lengths and to the complexation energies. In a previous work dedicated to the lead isoelectronic series,<sup>61</sup> we showed that the metal orbitals involved are the full 5d orbital and the empty 6p orbitals. The valence s orbitals are full and do not have proper symmetry to allow backdonation. The bonding

TABLE IX. Energy decompositions at the B3LYP/DEF2 level (kcal mol<sup>-1</sup>).

	[Pt(CO)]	[Au(CO)] <sup>+</sup>	[Hg(CO)] <sup>2+</sup>	[Tl(CO)] <sup>3+</sup>
$\Delta E_{AB}$	-79.3	-48.6	-83.2	-175.7
E <sub>1</sub>	150.1	56.3	9.8	-8.7
E <sub>2</sub>	-196.6	-97.8	-92.1	-166.6
$\delta E$	-32.8	-7.1	-1.0	-0.4
Cation polarization	-47.5	-19.8	-8.3	-6.1
CT: cation to CO	-60.4	-18.9	-3.4	-0.6
CO polarization	-33.2	-15.3	-38.6	-74.6
CT: CO to cation	-55.4	-43.8	-41.9	-85.3

was shown to be ensured by ligand polarization and donation toward the cation; relativistic effects were found to remain weak for both properties.

In this paper, we have studied the gold isoelectronic series that exhibits full 5d orbitals as HOMO and an empty 6s orbital as LUMO. We retrieved the special sensitivity of Au<sup>+</sup> toward relativity. The scalar CSOV energy decomposition and full relativistic computations show that this is due to the simultaneous relativistic expansion of the 5d orbitals and to the contraction of the 6s orbital in order to maximize the donation and the backdonation between the cation and the CO ligand. This particular synergy fades away with mercury and thallium: as *Z* increases, the 5d orbitals are more and more contracted and backdonation vanishes. At this point, the coordination becomes governed by the accepting 6s orbitals only and starts to be less sensitive to the relativistic effects. The relativistic effects are more important for the gold series than for the lead series because gold active 5d and 6s orbitals are more affected by relativity than the active 6p orbitals of lead. We have previously observed<sup>61</sup> that the element below Pb in the Periodic Table, namely, ununquadium, is very sensitive to the relativistic effects: the equivalent for Au, namely, roentgenium, will also probably exhibit a very intriguing behavior. Such results could also be useful for the design of accurate new generation force fields dedicated to such metal cations.<sup>63–65</sup>

- <sup>1</sup>D. J. Gorin and F. D. Toste, *Nature (London)* **446**, 395 (2007).
- <sup>2</sup>P. Pyykkö, *Chem. Soc. Rev.* **37**, 1967 (2008).
- <sup>3</sup>P. Pyykkö and J. P. Desclaux, *Acc. Chem. Res.* **12**, 276 (1979).
- <sup>4</sup>J. P. Desclaux, *At. Data Nucl. Data Tables* **12**, 311 (1973).
- <sup>5</sup>C. Gourlaouen, J.-P. Piquemal, T. Saue, and O. Parisel, *J. Comput. Chem.* **27**, 142 (2006).
- <sup>6</sup>A. Dedieu, *Chem. Rev. (Washington, D.C.)* **100**, 543 (2000).
- <sup>7</sup>K. Faegri, *Theor. Chem. Acc.* **105**, 252 (2001).
- <sup>8</sup>DIRAC, a relativistic *ab initio* electronic structure program, Release DIRAC04 (2004), written by H. J. Aa. Jensen, T. Saue, and L. Visscher with contributions from V. Bakken, E. Eliav, T. Enevoldsen, T. Fleig, O. Fossgaard, T. Helgaker, J. Laerdahl, C. V. Larsen, P. Norman, J. Olsen, M. Perpointner, J. K. Pedersen, K. Ruud, P. Salek, J. N. P. van Stralen, J. Thyssen, O. Visser, and T. Winther, see <http://dirac.chem.sdu.dk>.
- <sup>9</sup>T. Saue and T. Helgaker, *J. Comput. Chem.* **23**, 814 (2002).
- <sup>10</sup>O. Fossgaard, O. Gropen, M. Corral Valero, and T. Saue, *J. Chem. Phys.* **118**, 10418 (2003).
- <sup>11</sup>L. Visscher and T. Saue, *J. Chem. Phys.* **113**, 3996 (2000).
- <sup>12</sup>L. Visscher and K. G. Dyall, *At. Data Nucl. Data Tables* **67**, 207 (1997).
- <sup>13</sup>L. Visscher, *Theor. Chem. Acc.* **98**, 68 (1997).
- <sup>14</sup>J.-M. Lévy-Leblond, *Commun. Math. Phys.* **6**, 286 (1967).
- <sup>15</sup>GAUSSIAN 03, Revision C.02, M. J. Frisch, G. W. Trucks, H. B. Schlegel *et al.*, Gaussian, Inc., Wallingford, CT, 2004.
- <sup>16</sup>C. Lee, W. Yang, and R. G. Parr, *Phys. Rev. B* **37**, 785 (1988).
- <sup>17</sup>A. D. Becke, *J. Chem. Phys.* **98**, 5648 (1993).
- <sup>18</sup>T. H. Dunning, *J. Chem. Phys.* **100**, 2975 (1989).
- <sup>19</sup>F. Weigend and R. Ahlrichs, *Phys. Chem. Chem. Phys.* **7**, 3297 (2005).
- <sup>20</sup>E. Reed, R. B. Weinstock, and F. Weinhold, *J. Chem. Phys.* **83**, 735 (1985).
- <sup>21</sup>P. S. Bagus, K. Hermann, and C. W. Bauschlicher, Jr., *J. Chem. Phys.* **80**, 4378 (1984).
- <sup>22</sup>P. S. Bagus, K. Hermann, and C. W. Bauschlicher, Jr., *J. Chem. Phys.* **81**, 1966 (1984).
- <sup>23</sup>P. S. Bagus and F. Illas, *J. Chem. Phys.* **96**, 8962 (1992).
- <sup>24</sup>W. J. Stevens and W. H. Fink, *Chem. Phys. Lett.* **139**, 15 (1987).
- <sup>25</sup>K. Morokuma, *Acc. Chem. Res.* **10**, 294 (1977).
- <sup>26</sup>K. Kitaura and K. Morokuma, *Int. J. Quantum Chem.* **10**, 325 (1976).
- <sup>27</sup>J.-P. Piquemal, R. Chelli, P. Procacci, and N. Gresh, *J. Phys. Chem. A* **111**, 8170 (2007).
- <sup>28</sup>G. te Velde, F. M. Bickelhaupt, E. J. Baerends, C. Fonseca Guerra, S. J. A. Van Gisbergen, J. G. Snijders, and T. Ziegler, *J. Comput. Chem.* **22**, 931 (2001).
- <sup>29</sup>F. M. Bickelhaupt and E. J. Baerends, *Rev. Comput. Chem.* **15**, 1 (2000).
- <sup>30</sup>T. Ziegler and A. Rauk, *Inorg. Chem.* **18**, 1755 (1979).
- <sup>31</sup>G. A. Cisneros, T. A. Darden, N. Gresh, P. Reinhardt, O. Parisel, J. Pilmé, and J.-P. Piquemal, in *Multi-Scale Quantum Models for Biocatalysis: Modern Techniques and Applications*, Challenges and Advances in Computational Chemistry and Physics, edited by D. M. York and T.-S. Lee (Springer, New York, 2009), pp. 137–172.
- <sup>32</sup>M. Dupuis, A. Marquez, and E. R. Davidson, HONDO95.3, Quantum Chemistry Program Exchange (QCPE), Indiana University, Bloomington, IN 47405.
- <sup>33</sup>J.-P. Piquemal, A. Marquez, O. Parisel, and C. Giessner-Prettre, *J. Comput. Chem.* **26**, 1052 (2005).
- <sup>34</sup>K. Morokuma, *J. Chem. Phys.* **55**, 1236 (1971).
- <sup>35</sup>M. S. Gordon and J. H. Jensen, in *Encyclopedia of Computational Chemistry*, edited by P. von Ragué Schleyer (Wiley, Chichester, 1998), Vol. 5, pp. 3198–3214.
- <sup>36</sup>M. Neyman, S. Ph. Ruzankin, and N. Rösch, *Chem. Phys. Lett.* **246**, 546 (1995).
- <sup>37</sup>S. C. Chung, S. Kruger, S. Ph. Ruzankin, G. Pacchioni, and N. Rösch, *Chem. Phys. Lett.* **248**, 109 (1996).
- <sup>38</sup>A. M. Márquez, N. López, M. García-Hernández, and F. Illas, *Surf. Sci.* **442**, 463 (1999).
- <sup>39</sup>A. Ricca and C. W. Bauschlicher, *J. Phys. Chem. A* **106**, 3219 (2002).
- <sup>40</sup>D. Schröder, H. Schwarz, J. Hrušák, and P. Pyykkö, *Inorg. Chem.* **37**, 624 (1998).
- <sup>41</sup>C. Gourlaouen, J.-P. Piquemal, and O. Parisel, *J. Chem. Phys.* **124**, 174311 (2006).
- <sup>42</sup>B. Liang, M. Zhou, and L. Andrews, *J. Phys. Chem. A* **104**, 3905 (2000).
- <sup>43</sup>L. Manceron, B. Tremblay, and M. E. Alikhani, *J. Phys. Chem. A* **104**, 3750 (2000).
- <sup>44</sup>C. J. Evans and M. C. L. Gerry, *J. Phys. Chem. A* **105**, 9659 (2001).
- <sup>45</sup>M. Zhou, L. Andrews, and C. W. Bauschlicher, *Chem. Rev. (Washington, D.C.)* **101**, 1931 (2001).
- <sup>46</sup>E. Yamazaki, T. Okabayashi, and M. Tanimoto, *Chem. Phys. Lett.* **396**, 150 (2004).
- <sup>47</sup>C. M. Rohlfing and P. J. Hay, *J. Chem. Phys.* **83**, 4641 (1985).
- <sup>48</sup>M. Ohno and W. von Niessen, *Phys. Rev. B* **45**, 9382 (1992).
- <sup>49</sup>S. Roszak and K. Balasubramanian, *J. Phys. Chem.* **97**, 11238 (1993).
- <sup>50</sup>S.-C. Chung, S. Krüger, G. Pacchioni, and N. Rösch, *J. Chem. Phys.* **102**, 3695 (1995).
- <sup>51</sup>A. J. Lupinetti, V. Jonas, W. Thiel, S. H. Strauss, and G. Frenking, *Chem.-Eur. J.* **5**, 2573 (1999).
- <sup>52</sup>Z. J. Wu, H. L. Li, H. J. Zhang, and J. Meng, *J. Phys. Chem. A* **108**, 10906 (2004).
- <sup>53</sup>M. Patzschke and P. Pyykkö, *Chem. Commun. (Cambridge)* **2004**, 1982.
- <sup>54</sup>P. K. Hurlburt, J. J. Rack, J. S. Luck, S. F. Dec, J. D. Webb, O. P. Anderson, and S. H. Strauss, *J. Am. Chem. Soc.* **116**, 10003 (1994).
- <sup>55</sup>B. Liang and L. Andrews, *J. Phys. Chem. A* **104**, 9156 (2000).
- <sup>56</sup>J. Velasquez, B. Njegic, M. S. Gordon, and M. A. Duncan, *J. Phys. Chem. A* **112**, 1907 (2008).
- <sup>57</sup>K. Mogi, Y. Sakai, T. Sonoda, Q. Xu, and Y. Souma, *J. Phys. Chem. A* **107**, 3812 (2003).
- <sup>58</sup>P. Pyykkö and N. Runeberg, *Asian J. Chem.* **1**, 623 (2006).
- <sup>59</sup>F. Tielens, L. Gracia, V. Polo, and J. Andrés, *J. Phys. Chem. A* **111**, 13255 (2007).
- <sup>60</sup>J. Hrušák, R. H. Hertwig, D. Schröder, P. Schwerdtfeger, W. Koch, and H. Schwarz, *Organometallics* **14**, 1284 (1995).
- <sup>61</sup>C. Gourlaouen, O. Parisel, and J.-P. Piquemal, *Chem. Phys. Lett.* **469**, 38 (2009).
- <sup>62</sup>See supplementary material at <http://dx.doi.org/10.1063/1.3491266> for the radii of the 5d and 6s shells of the neutral atoms at the FR-RHF and NR-RHF (in parentheses) levels.
- <sup>63</sup>N. Gresh, G. A. Cisneros, T. A. Darden, and J.-P. Piquemal, *J. Chem. Phys.* **3**, 1960 (2007).
- <sup>64</sup>J.-P. Piquemal, L. Perera, G. A. Cisneros, P. Ren, L. G. Pedersen, and T. A. Darden, *J. Chem. Phys.* **125**, 054511 (2006).
- <sup>65</sup>J.-P. Piquemal, G. A. Cisneros, P. Reinhardt, N. Gresh, and T. A. Darden, *J. Chem. Phys.* **124**, 104101 (2006).